AMERICAN JOURNAL OF INDUSTRIAL MEDICINE 30:515–528 (1996)

Mineral Phases and Some Reexamined Characteristics of the International Union Against Cancer Standard Asbestos Samples

Norihiko Kohyama, PhD, Yasushi Shinohara, PhD, and Yasunosuke Suzuki, MD

Standard asbestos samples to be used for biomedical research were first prepared by the International Union Against Cancer (UICC) in 1966 in the United Kingdom and South Africa. Using modern techniques. X-ray diffractometry. analytical transmission electron microscopy, and thermal analysis, we have now analyzed these UICC samples to determine the mineral compositions (mineral phases) and their respective quantities. UICC chrysotile A (from Zimbabwe) contains 2% fibrous anthophyllite as impurity; chrysotile B (from Canada) does not contain any fibrous impurities, only non-fibrous minerals. UICC amosite and crocidolite are almost pure. UICC anthophyllite has 20–30% talc as impurity. The chemical compositions and fiber size distributions of the UICC asbestos samples have also been determined. The mean widths of the fibers of chrysotile A and B are smaller than those of the amphibole fibers. This agrees well with the earlier results which showed the two chrysotile samples to have a larger respirable fraction than the amphiboles. © 1996 Wiley-Liss, Inc.

KEY WORDS: asbestos, standards, mineralogy, X-ray diffractometry, chrysotile, anthophyllite, amosite, crocidolite

INTRODUCTION

The four main types of asbestos (chrysotile A and B, crocidolite, amosite, and anthophyllite) were prepared for standard reference samples by the collaborative efforts of the Llandough Hospital MRC Pneumoconiosis Unit in the United Kingdom and the Pneumoconiosis Research Unit of the National Research Institute for Occupational Diseases in South Africa in 1966 [Timbrell and Rendall, 1972; Rendall, 1970; Timbrell, 1970] following the recommendations made after the Conference on the Biological Effects of Asbestos held in New York in 1964. Since then, these asbestos samples prepared by the International Union Against Cancer (UICC) have been used extensively in many important biomedical studies.

The chemical and physical characteristics of the prepared samples were initially and carefully determined [Rendall, 1970; Timbrell, 1970]. However, the mineral phases occurring as impurities were not determined and no data have been obtained on the actual asbestos percentage in each sample nor on the types and concentrations of all impurity minerals [Graf et al., 1982].

Recently it has been argued that chrysotile asbestos contains impurities, especially fibrous tremolite. This is an important argument because some fibrous tremolite has a strong carcinogenic action as shown in animal experimentation [Wagner et al., 1973, 1982]. Such contamination could adversely affect any experimental results when the UICC asbestos samples had been used.

For these reasons, it is important to know the type and quantity of mineral impurities in the UICC asbestos samples, especially if different kinds of fibrous minerals themselves exist as such impurities. This paper presents the de-

National Institute of Industrial Health, Ministry of Labour, Kawasaki, Japan (N.K., Y.Sh.).
Division of Environmental and Occupational Medicine, Mount Sinai School of Medicine of the City University of New York, New York (Y.Su.).
Address reprint requests to Dr. Norihiko Kohyama, National Institute of Industrial Health, Ministry of Labour, 21-1 Nagao 6 Chome, Tama-ku, Kawasaki 214, Japan.

Accepted for publication March

TABLE I. UICC Standard Asbestos Samples

Chrysotile A	(from Zimbabwe)
Chrysotile B	(from Canada)
Crocidolite	(from South Africa)
Amosite	(from South Africa)
Anthophyllite	(from Finland)

tails of the mineral phases of each UICC asbestos sample as well as the chemical and physical characteristics using modern instruments and techniques.

MATERIALS AND METHODS

Mineral Phases

To know the mineral phases, the UICC asbestos samples were determined by a conventional X-ray powder diffractometer (Rint 2200, Rigaku Co., Japan) equipped with a Cu X-ray tube (1.5 kV) and a graphite monochrometer. The powder sample embedded in Al-specimen holder was analyzed at a power of 40 kV and 30 mA with a scanning speed of 1°/min for diffraction angle from 2° to 70° and a step scanning (0.02° interval: 50 and 100 sec exposures for each step) for the detection of amphibole phases. These data were treated by an attached computer. To identify the minor mineral phases effectively, a computer was employed for matching the X-ray diffraction (XRD) peaks with the mineral powder diffraction file.[1] In this matching analysis, as the peak intensities were expressed in the square root, i.e., small peaks were enlarged and large peaks shrunk in one XRD pattern, all minor phases could be successively identified with high precision.

XRD patterns for the UICC asbestos samples are shown in Figures 1 and 2. Figure 1 shows the XRD patterns of chrysotile A and B, of which low diffraction angle parts (5–50° in 2Θ) were enlarged in Figure 1 (bottom) to show the minor mineral phases present in the two chrysotile samples. Figure 2 shows the XRD patterns of the UICC amphibole asbestos samples. The peaks of coexisting minerals (impurity minerals) were indicated on the figures of each sample. The precise data of each XRD peak, such as 2Θ, d-spacing, intensity, identification, and Miller index, are omitted here. Table II shows the mineral phases identified and quantified in the five UICC standard asbestos samples by XRD, combined with analytical transmission electron microscopy (ATEM). The detection limit of the XRD analysis was about 0.5% in weight.

Small amounts of other minerals were identified as impurities in chrysotile A (from Zimbabwe) and chrysotile B (from Canada). Anthophyllite was found in chrysotile A by XRD and was identified as fibrous by ATEM. Since strong and major XRD peaks of talc are overlapped with some peaks of anthophyllite, the presence of talc was also examined by ATEM for chrysotile A and talc was confirmed showing irregular platy shape. The finding of anthophyllite in chrysotile A will be discussed further. No tremolite peak was detected in either of the chrysotile samples. Although we also examined the chrysotile samples for the presence of tremolite more precisely by XRD analysis employing a step scanning method, no tremolite peak was detected at the detection level of 0.1%. The other identified minerals were all non-fibrous minerals, mostly of platy morphology.

Quantification of coexisting minerals in the two UICC chrysotile samples showed that they exist in very small amounts judging from the XRD patterns. The amounts of each mineral, such as anthophyllite, brucite, and pyroaurite in chrysotile A and B, were estimated by an internal standard method using pure powdered quartz (from Fukushima, Japan) as an internal standard. Pure (or mostly pure) samples of anthophyllite (from Afghanistan; fibrous), brucite (from China; platy) and pyroaurite (from Norway; platy) were used for the standard minerals allowing the calibration lines for each mineral to be quantified. The quartz powder was added into the UICC chrysotile samples and the samples of the standard anthophyllite, brucite, and pyroaurite at 10% in weight. The ratio of a peak intensity of each mineral to that of quartz was measured for each sample. Then, the calibration lines were made by connecting the intensity ratio with the origin of the coordinate axes by a straight line for each mineral. By this XRD quantification, the quantity of anthophyllite in chrysotile A was estimated to be 3% by weight. However, this percentage also contains a small amount of talc and the actual content of anthophyllite was estimated as approximately 2% on the basis of the ATEM observation. The other minerals present were also quantified, as shown in Table II; the contents of chrysotile in the samples of chrysotile A and B were 94% and 92%, respectively.

Some very weak peaks of quartz, estimated at about 1% or less by weight (Fig. 2), were identified in the amosite and crocidolite samples. No other peaks were found. In the anthophyllite sample, talc, chlorite, and mica (probably phlogopite) were identified (Fig. 2). The chlorite and mica were estimated as being about 5%, respectively. It was found that the UICC anthophyllite sample contains substantial talc according to the ATEM observation. In order to estimate this amount of talc, the XRD pattern of the UICC anthophyllite sample was compared with those of other fibrous anthophyllite samples (Figure 3). Fibrous anthophyllite from Afghanistan is mostly pure, but a very small amount of talc was found by ATEM. Fibrous anthophyllite from Uchida, Japan, also has a small amount of talc, but the amount seemed to be much smaller than that of the UICC antho-

1. Published by the Joint Committee of Powder Diffraction Standards (JCPDS)-International Centre for Diffraction Data (ICDD), 1993.

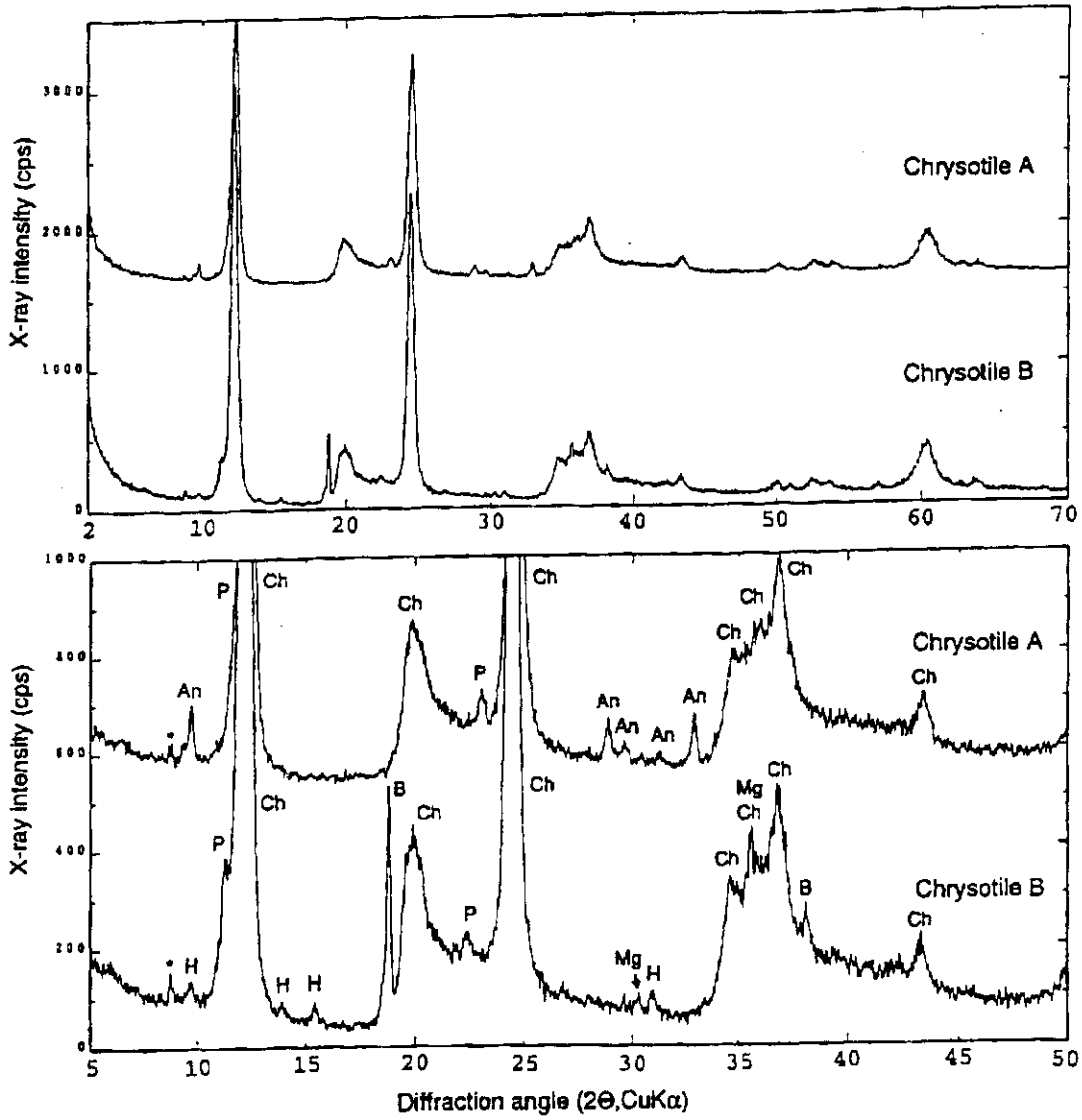

FIGURE 1. XRD patterns of the UICC chrysotile samples. Ch, chrysotile; An, anthophyllite; P, pyroauxite; H, hydromagnesite; B, brucite; Mg, magnetite; *, noise peak from specimen holder.

phyllite. It also has a very small amount of vermiculite. The identification and quantification of talc in anthophyllite sample by XRD are very difficult because strong major peaks of 9.4, 4.67, and 3.12 Å of talc are all overlapped with those of anthophyllite. In addition, the orientation effect of fibrous anthophyllite is obviously large. Conversely, the detection and quantification of anthophyllite in talc by XRD are easier as reported [Rohl and Langer, 1974]. We are trying to develop a precise method for quantification of talc in anthophyllite, but by the present rough estimation, the UICC anthophyllite sample appears to contain over 20% of talc as impurity at least. The shapes of talc particles were mostly irregular platy ones, but some of them showed lath or fibrous shapes. As the fibrous talc could be misunder-

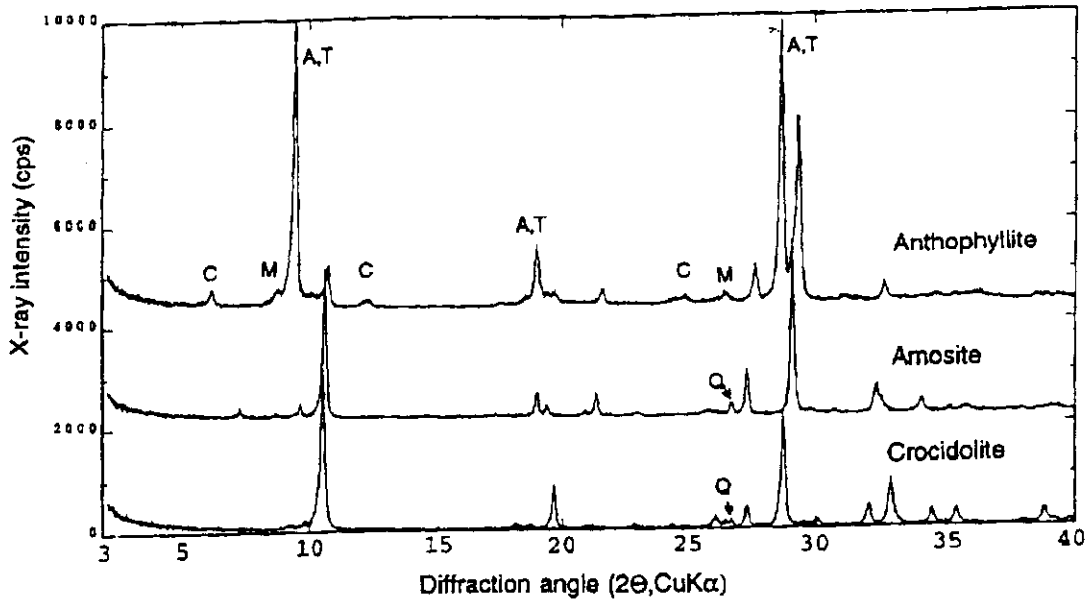

FIGURE 2. XRD patterns of the UICC amphibole asbestos samples. C, chlorite; M, mica (phlogopite); A, T, overlapped peak of anthophyllite and talc; Q, quartz.

TABLE II. Mineral Phases of the UICC Standard Asbestos Samples Determined by XRD Analysis and Some Other Methods

	Weight (%)			Weight (%)			Weight (%)
Minerals	Chrysotile A	Chrysotile B	Minerals	Amosite	Crocidolite	Minerals	Anthophyllite
Chrysotile	94	92[a]	Amosite	99	—	Anthophyllite	60
Anthophyllite	2	—	Crocidolite	—	99	Talc	30
Talc	1[a]	—	Quartz	<1	<1	Chlorite	5
Brucite	—	6				Phlogopite	5
Lizardite	—	Trace[b]					
Antigorite	<1[a]	Trace[b]					
Pyroaurite[c]	2	2					
Hydromagnesite[d]	—	Trace[b]					
Magnetite	—	Trace[b]					
Total (%)	100	100		100	100		100

[a]Including 6-layer serpentine at approximately 1%.
[b]Identified and estimated by ATEM analysis. Trace, <0.5%.
[c]Pyroaurite, $Mg_6Fe_2CO_3(OH,Cl)$ 16.4 H_2O, platy mineral.
[d]Hydromagnesite, $Mg_5(CO_3)_4(OH)$ 2.4 H_2O, platy mineral.

stood as fibrous anthophyllite, the precise identification by ATEM is required. The content of the talc was also estimated by chemical analysis.

Chemical Composition

Major elements of the UICC asbestos samples were analyzed by gravimetric determination for SiO_2 and Fe_2O_3 + Al_2O_3, colorimetric methods for FeO, and inductively coupled plasma-atomic emission spectrometry and atomic absorption spectrometry for TiO_2, Fe_2O_3, MnO, MgO, CaO, Na_2O, and K_2O. The other minor elements were determined by X-ray fluorescence analysis for their presence and quantities.

The results of our analyses of the chemical composition

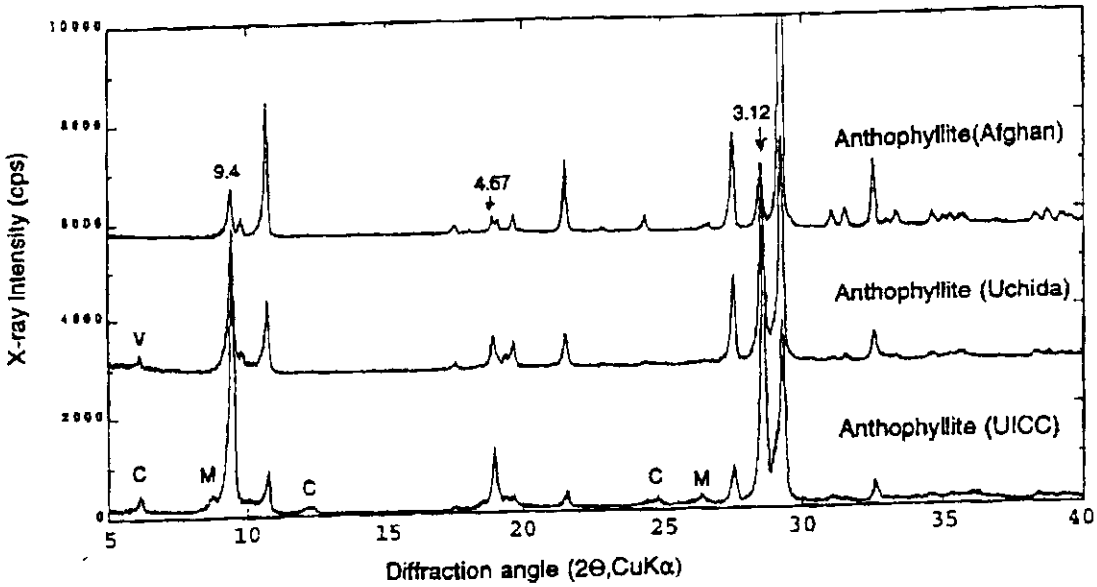

FIGURE 3. XRD patterns of the UICC anthophyllite sample and of the other localities. Numbers, d-spacing in Å: V, vermiculite; C, chlorite; M, mica (phlogopite).

of the UICC asbestos samples are given in Table III. Traditionally, the cations of silicate minerals have been expressed in oxide percent. The chemical compositions of the UICC asbestos samples were reported on earlier by Timbrell [1970]; since the expression of those results was slightly different from the traditional way, they could not be compared with our present data.

For chrysotile A and B, the chemical compositions are close to ideal: the contents of MgO and $H_2O(+)$ in chrysotile B were slightly larger, which may be due to brucite [$Mg(OH)_2$] as an impurity. Part of the iron content will be in the chrysotile structure itself but part can also be attributed to the impurities, pyroaurite and magnetite.

The amosite and crocidolite samples showed a typical chemical composition for these minerals, which means the samples are mostly pure. It is a characteristic of amosite and crocidolite to contain small amounts of Mn and Na ions, respectively.

As minor elements, very small amounts of Cr and Ni ions were present in the samples of chrysotile and anthophyllite. These are considered to replace the Mg ions in the crystal structures.

An ideal anthophyllite mainly consists of Si, Mg, and a small amount of Fe for the cations. The anthophyllite sample, however, had noticeably high contents of Al_2O_3 and K_2O. These latter correspond well with the presence of chlorite and mica (phlogopite) as impurities. The amount of the actual hydroxyl water, which was estimated to be 3.65%, was also larger than that of anthophyllite (calculated as 2.3% for the ideal crystal structure). The estimation of the actual hydroxyl water is described below.[2] These results reflect the fact that the UICC anthophyllite sample contains talc, chlorite, and phlogopite as impurities. These minerals' ideal amounts of hydroxyl water are larger than that of anthophyllite, i.e., 4.7%, 13%, and 4.3%, respectively. Using these values of ideal hydroxyl water, the contents of each mineral can be calculated as anthophyllite 60%, talc 30%, chlorite 5%, and mica 5% by the following equation:

$$2.3(\%)\ A + 4.7(\%)\ T + 13(\%) \times C + 4.3(\%) \times M = 3.65(\%)$$

where A, T, C, and M are the fractions of anthophyllite, talc, chlorite, and mica, respectively, and $T = 1.0 - A - C - M$, as the fractions of chlorite (C) and mica (M) had been

2. As the iron in the original anthophyllite sample was all oxidized when heated at 1,100°C (ignition) to measure the content of $H_2O(+)$, the value of hydroxyl water was measured smaller by the weight gain following the oxidation. To subtract the weight gain and obtain the actual content of hydroxyl water, the total iron was initially expressed by a ferric form as in the parentheses in Table III, then only the ferric iron was recalculated into ferrous form and the weight difference (6.32 − 5.75 = 0.57%) was added to the initial value of $H_2O(+)$: 3.65% producing 4.22%. Finally, the actual content of hydroxyl water could be estimated to be 3.65% by subtracting the value of SO_2: 0.57%, which was recalculated from SO_3:0.71% and was considered to be contained in the initial weight loss of $H_2O(+)$:3.65% as a gas component, from that of $H_2O(+)$:4.22%.

TABLE III. Chemical Compositions of the UICC Standard Asbestos Samples*

	Chrysotile A	Chrysotile B	Amosite	Crocidolite	Anthophyllite
SiO_2	39.89	38.10	50.53	48.84	55.31
TiO_2	0.02	Trace	ND	0.02	0.03
Al_2O_3	0.76	0.40	0.55	0.06	0.99
Fe_2O_3	1.97	2.39	1.90	19.07	(6.32)
FeO	0.49	1.14	35.34	19.95	5.75
MnO	0.06	0.06	1.82	0.11	0.17
MgO	42.60	43.26	6.43	2.32	31.15
CaO	0.33	0.17	0.51	1.08	0.29
Na_2O	Trace	0.02	0.02	5.58	0.03
K_2O	Trace	0.02	0.27	0.06	0.43
$H_2O(+)$	12.58	13.67	2.32	2.33	(3.65) 4.22
$H_2O(-)$	0.87	0.66	0.20	0.34	1.31
Minor elements					
SO_3†	0.31	0.13	0.24	0.03	0.71
Cl†	0.05	0.25	0.03	Trace	0.01
Cr_2O_3	0.23	0.07	Trace	ND	0.13
Co_2O_3	Trace	Trace	ND	ND	Trace
NiO	0.21	0.12	Trace	Trace	0.14
CuO	ND	ND	ND	ND	Trace
ZnO	Trace	Trace	ND	ND	0.03
Total (%)	100.01	100.08	99.93	99.76	100.00

*Data obtained by wet chemical analyses except for anthophyllite and minor elements, which were obtained by X-ray fluorescence spectrometry. Trace, <0.01%; ND, not detected (<0.001); numbers in parentheses, see text. $H_2O(+)$ and $H_2O(-)$, weight loss by ignition up to 1,100°C and 110°C, respectively.
†These values included in $H_2O(+/-)$ and excluded from the total.

obtained earlier by XRD analyses as 0.05, respectively (Table II), T = (0.9 − A). From this, the above equation can be written:

$$2.3(\%)\ A + 4.7(\%)(0.9 - A) + 13(\%) \times 0.05 + 4.3(\%) \times 0.05 = 3.65(\%).$$

Therefore, the fraction of anthophyllite (A) can be calculated to be 0.60, and that of talc 0.30. This calculation has a relatively large error, but can be used to estimate the approximate content of talc.

Thermal Analysis

Thermal analysis can indicate various kinds of thermal reactions of minerals, such as dehydration of absorption water, surface water, and interlayer water (occurring at approximately 100–140°C), dehydroxidation of structural water (OH), oxidation of ferrous iron, phase transformation, etc., which are unique for each mineral. The differential thermal analysis (DTA), thermal gravimetry (TG), and derivative thermal gravimetry (DTG) were simultaneously done using a DTA-TG apparatus (Thermoflex TAS300, Rigaku Co.) for the UICC asbestos samples. The heating rate and sample weight were 20°C/min and approximately 20 mg, respectively. To prevent the oxidation of ferrous iron contained in the amosite and crocidolite, the thermal analyses were also done in an N_2 environment in addition to the normal analyses in air. The results are shown in Figure 4.

In the DTG curves of chrysotile A and B, the peaks of 665°C and 650°C show the dehydroxidation of OH water in chrysotile. Exothermic peaks of 837°C and 831°C in the DTA curves of chrysotile A and B show the recrystallization to forsterite and/or enstatite from the amorphous state after the dehydroxidation. The other peaks in the DTG curves would indicate that minor minerals coexisted: 260°C (pyroaurite), 372°C (brucite), 580°C and 560°C (probably chlorite), and 712°C (antigorite).

FIGURE 4. DTA and DTG curves of the UICC standard asbestos samples. In air, analyzed in air environment; in N_2 analyzed in N_2 environment; A and B, chrysotile A and B, respectively.

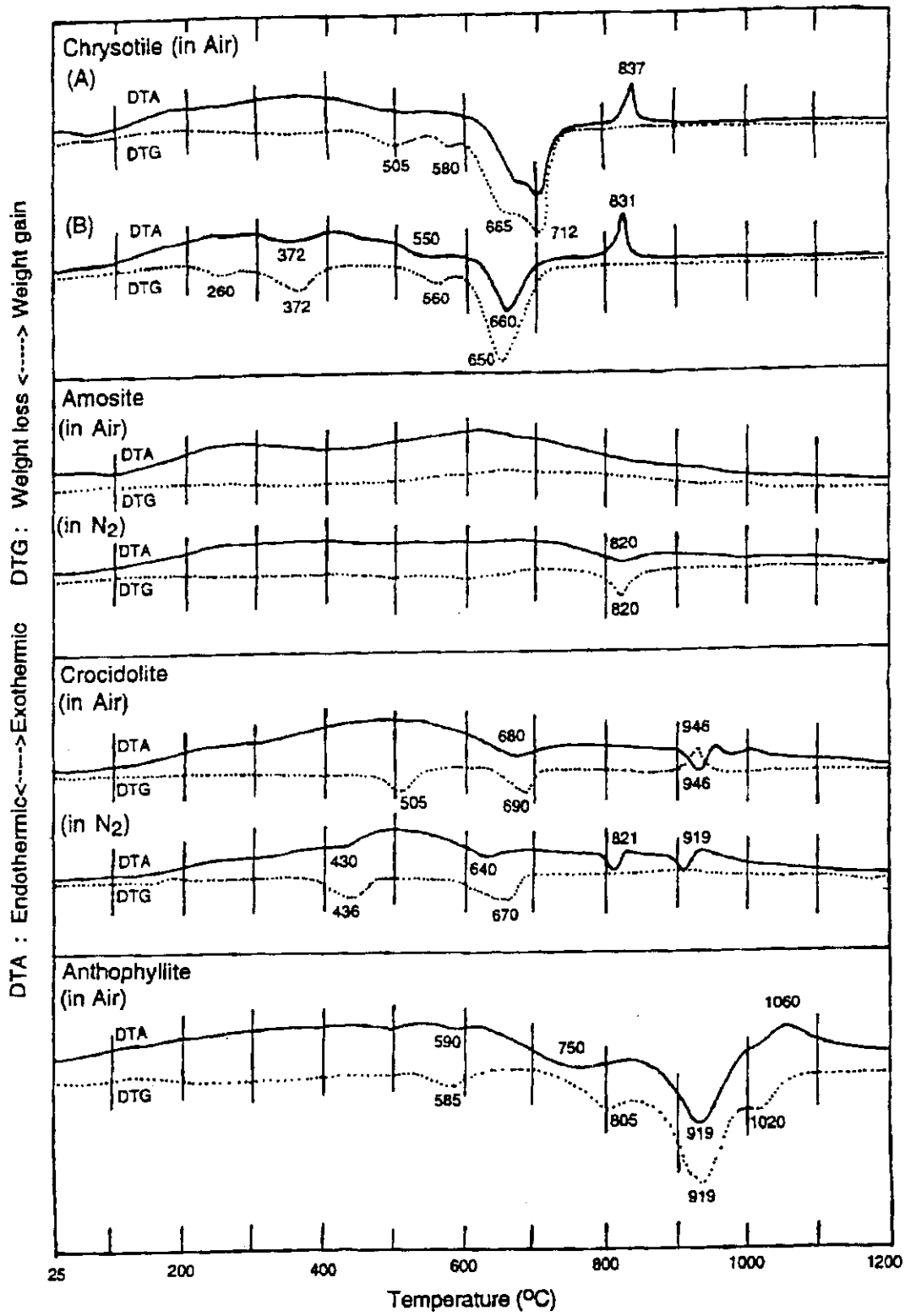
Chrysotile (in Air)
(A)
DTA
DTG
837
505
580
665
712
(B)
DTA
DTG
831
550
372
260
372
560
660
650
Amosite
(in Air)
DTA
DTG
(in N2)
DTA
DTG
820
820
Crocidolite
(in Air)
DTA
DTG
680
946
946
505
690
(in N2)
DTA
DTG
430
436
640
670
821
919
Anthophyllite
(in Air)
DTA
DTG
590
585
750
805
919
919
1060
1020
DTA : Endothermic<----->Exothermic DTG : Weight loss <----> Weight gain
25
200
400
600
800
1000
1200
Temperature (°C)

FIGURE 4.

The DTA and DTG curves of the amosite did not show any peaks in the air environment, but in the N_2 environment the endothermic peak and weight loss peak were detected at 820°C in the respective curves. The oxidation of ferrous iron in the amosite occurred at a relatively low temperature of approximately 400–500°C and continued gradually up to 1,000°C or more in air. The DTG curve shows a broad weight gain curve between approximately 500 and 1,000°C. No mineral impurity was detected in the amosite sample by the thermal analysis. The final products of the amosite, as determined by XRD after heating to 1,200°C in an air environment, were quartz and cristobalite (SiO_2), magnetite ($FeO{\cdot}Fe_2O_3$), hematite (Fe_2O_3), and enstatite ($MgSiO_3$), and in an N_2 environment were quartz, cristobalite, magnetite, and enstatite.

The DTA and DTG curves of crocidolite analyzed in both air and an N_2 environment were slightly different from each other. In air, the DTG curve showed weight loss peaks at 505°C and 690°C and a weight gain peak at 946°C, while the DTA curve showed endothermic peaks at only 680°C and 946°C. The low sensitivity of DTA is the reason why the endothermic peak at approximately 500°C was not detected. In N_2, the DTG curve showed two weight loss peaks at 436°C and 670°C which became slightly lower than those of in air. The weight gain did not occur at 946°C as in air. The DTA curve showed four endothermic peaks at 430°C, 640°C, 821°C, and 919°C. The first two endothermic peaks would show the dehydroxidation of hydroxyl water of the crocidolite. The oxidation of the ferrous iron would occur at about 946°C, corresponding to the weight gain and transformation of crystal structure. The endothermic peak of the DTA at 946°C would be due to the transformation. In N_2, the transformation occurred at 919°C, but the oxidation did not occur abruptly but proceeded gradually and the DTG curve did not show a clear weight gain peak at approximately 919°C. An endothermic peak newly appeared at 821°C in the DTA curve in N_2. The cause of the peak cannot be explained at the present. No mineral impurity was detected in the crocidolite sample by the thermal analysis. The final mineral products when heated in an air environment were quartz, cristobalite, and hematite. When heated in an N_2 environment, magnetite was found in addition to the other products.

The thermal analysis for anthophyllite showed complex curves of DTA and DTG disclosing some coexisting minerals. In the DTG curve, the peaks at 585°C, 805°C, 919°C, and 1,060°C would be derived from the dehydroxidation of structural water of chlorite, mica, anthophyllite, and talc, respectively. The DTA curve was mostly consistent with the DTG curve. The exothermic peak at approximately 1,060°C would be due to the transformation of the crystal structure. The final mineral products after heating to 1,200°C were quartz, cristobalite, and enstatite.

Transmission Electron Microscopic (TEM) Observation

ATEM analyses for the UICC asbestos samples were done using a TEM (H-8000, Hitachi Co., Japan) equipped with an energy dispersive X-ray spectrometer (EDX, Kevex Co., USA) at an accelerating voltage of 200 kV. The UICC asbestos samples were dispersed in pure water and a droplet of the dispersion was put on an Ni TEM grid with collodion film coated by carbon.

The TEM photographs for UICC asbestos samples are shown in Figure 5a–e. It can be seen that chrysotile A and B consist of very thin curly fibers (fibrils) as well as thicker fibers (fiber bundles). In both samples, platy minerals were also found, which were identified to be lizardite, antigorite, pyroaurite, brucite, chlorite, and talc as minor impurities on the basis of their selected area electron diffraction (SAED) patterns and EDX spectra. In chrysotile A, fibrous anthophyllite was also commonly found by TEM observation as impurity fibers. To observe the presence of anthophyllite fibers more clearly and the ratio to talc, the chrysotile fibers in chrysotile A were digested by a strong acid (HCl) and an alkaline (NaOH) solution, by which the minor minerals such as anthophyllite and talc were concentrated in the remainder as shown in Figure 6. The SAED pattern and EDX spectrum in Figure 6 proved the coexisting fibers are typical anthophyllite, showing an example of the chemical composition as SiO_2 56.5%, MgO 32.4%, and FeO 10.1%, which is also similar to that of UICC anthophyllite. The platy particles seen in Figure 6 were talc and the amount seemed to be much smaller than the anthophyllite fibers. The fibrous anthophyllite mostly consisted of relatively large fibers, such as 1–50 μm in length and 0.1–3 μm in diameter (Fig. 6).

In contrast to curly fibers of chrysotile, fibrous amphiboles usually show a rectilinear shape of the particles as seen in Figure 5c–e, which are UICC amosite, crocidolite, and anthophyllite, respectively. The amosite and crocidolite samples appeared almost pure by TEM observation, but the anthophyllite sample contained many platy minerals, which were mostly talc with some mica and chlorite. The talc particles occurred mostly as irregular plates, but fibrous talc was also found. Fibrous talc can be differentiated from fibrous anthophyllite by SAED or EDX analysis. Of the three examples of amphibole asbestos, fine fibers were common in the crocidolite sample.

Fiber Size Distributions

The fibers in all of the UICC asbestos samples obviously differ widely in aspect ratio (length and width), from very short and thin to very long and thick. To obtain the fiber size distribution, all of the fibers in a sample from

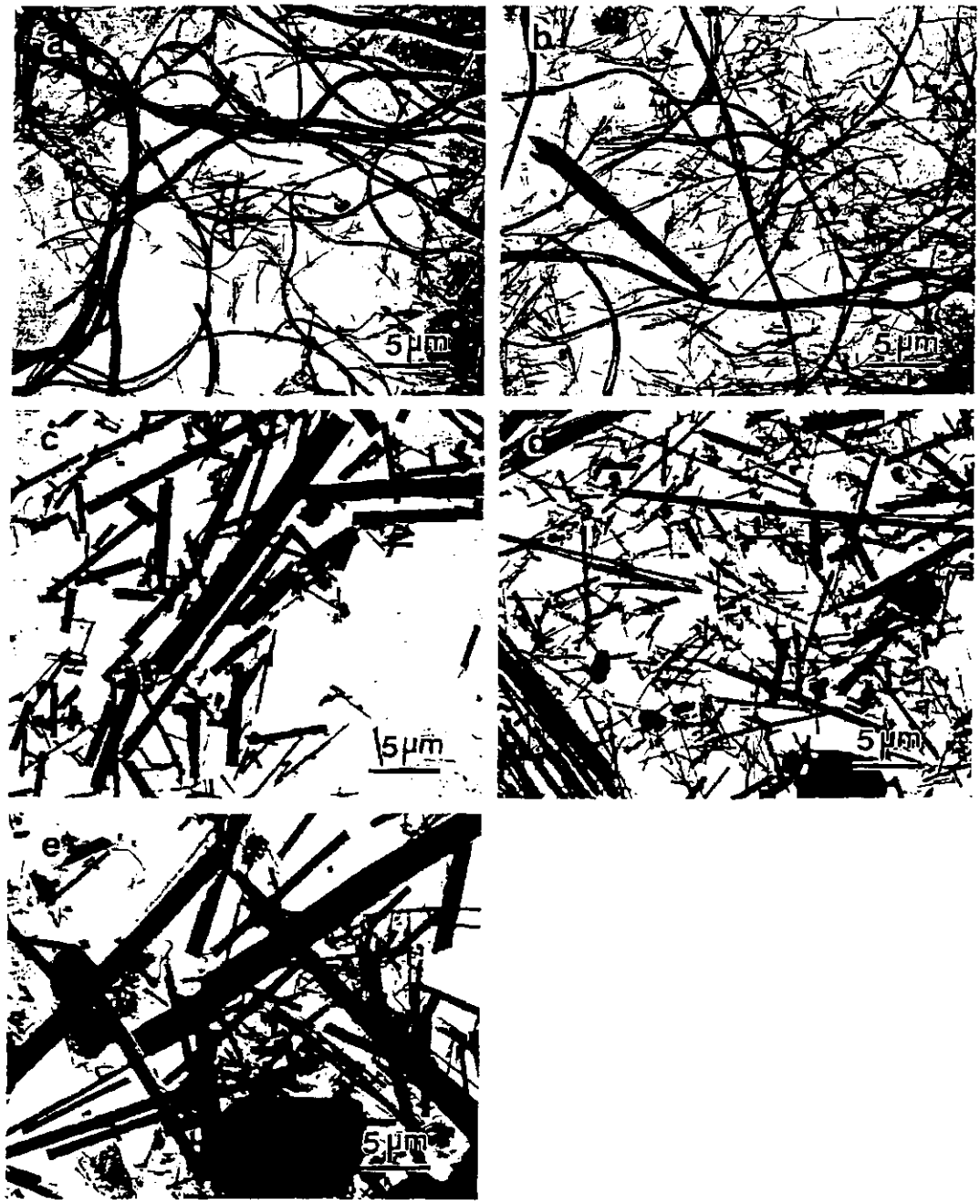

FIGURE 5. TEM photographs of the UICC asbestos samples. a: Chrysotile A. b: Chrysotile B. c: Amosite. d: Crocidolite. e: Anthophyllite.

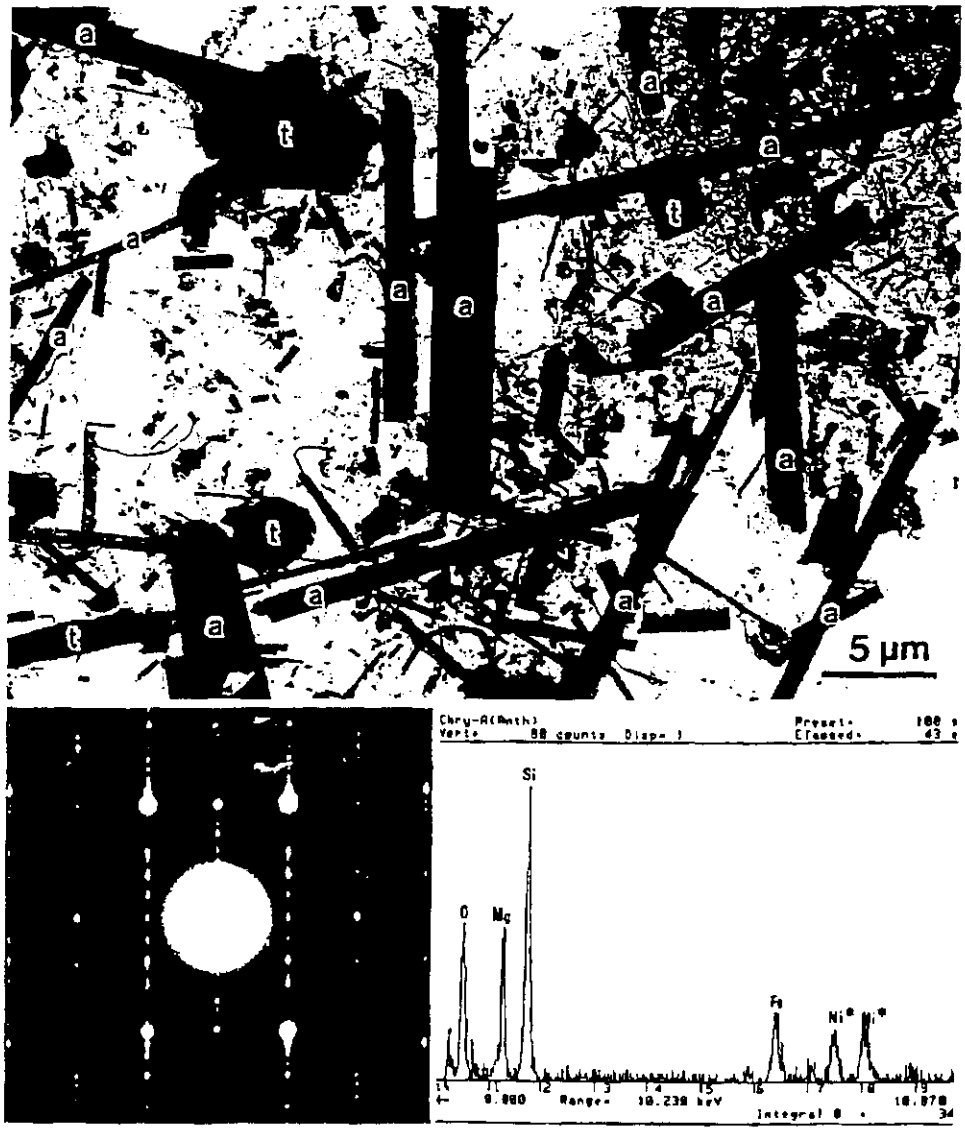

FIGURE 6. TEM photograph of the remainder of the chrysotile A sample chemically digested, showing anthophyllite fibers (a) and platy talc particles (t). The SAED pattern and EDX spectrum show that the fibers are a typical anthophyllite. Ni* in EDX spectrum, noise from Ni TEM grid.

short to long as well as from thin to thick must be examined by electron microscopy at a proper magnification. Some new TEMs having a very high resolution at low magnifications (less than ×100) have been developed recently. Two such TEMs having this ability, LEM-2000 (Topcon Co., Japan) and H-8000, were used in the present study for the measurement of fiber sizes.

The five UICC asbestos samples were well dispersed in distilled water and the proper portions were filtered on cellulose ester membrane filter (Millipore filter®). The mem-

brane filter samples were transferred onto TEM grids following low temperature ashing and carbon extraction techniques [Kohyama and Suzuki, 1991]. The TEM samples were observed using a TEM (LEM-2000 or H-8000), and the photographs were taken at magnifications of a few hundred times. The negatives were enlarged on the print by 10 times or more. The prints, therefore, had total magnifications of a few thousand times. Fiber lengths were measured using either a ruler or a scale magnifier of ×10 magnification, and the widths were measured by the scale magnifier on the prints. When the fiber size was measured by the scale magnifier, the size could be detected down to 0.01 μm at a total magnification of a few ten thousand times. The total number of fibers counted for the size measurement ranged from 300 to 500 fibers for each sample. The benefit of this method is that almost all fibers on a very wide field of the TEM sample could be observed on one print.

The data for fiber sizes were plotted on a log-normal distribution chart for each sample (Fig. 7a–e). The measured fiber size parameters such as geometrical mean and geometrical standard deviation (SD) for length and width are shown in Table IV. The mean lengths of the chrysotile A and B and crocidolite sample are slightly shorter than those of the amosite and anthophyllite samples. These also have a large SD, indicating large fiber length distributions. Length and width measurements were repeated on amosite and crocidolite samples from a different portion of our UICC samples. The results of these second measurements are shown in parentheses in Table IV. The variability in width and length is fairly large, which is to be expected from such mineral samples. Considering the observed variability, however, these results clearly show similar size distributions for UICC amosite and UICC crocidolite. This is in direct contrast with the photographs of samples of amosite and crocidolite pictured on page 296 of "Biological Effects of Asbestos," IARC Scientific Publication No. 8 [Bogovski et al., 1973]. The IARC publication suggests a severalfold thinner size distribution for crocidolite compared with amosite.

The fiber lengths of all five UICC samples had been measured earlier by Rendall [1970] and Timbrell [1970], and for comparison those data were also plotted in the same figures. The mean fiber widths are newly reported in this paper. Concerning the length distributions for all samples, the Rendall data (curve 1 in Fig. 7a–e), which combined both the data of optical microscopy (OM) and TEM, gave shorter lengths compared to those found in the present analyses. The 1970 Timbrell data on length by TEM for the airborne fibers (curve 3 in Fig. 7a–e) were also slightly shorter than those of ours for amphibole samples (but of similar length for chrysotile A and B samples). It is likely that the data of OM (curves 2 and 4 in Fig. 7a–e), which would measure fibers longer than 3 μm only, were biased to express a longer size range than those of the TEM.

The mean fiber widths of chrysotile A and B were less than those of the amphiboles; i.e., the mean fiber widths of the three amphibole samples were 0.31–0.38 μm, but 0.17 and 0.15 μm for chrysotile A and B. Timbrell [1970] reported that the two chrysotile samples (chrysotile A and B) would be more respirable than the amphiboles. The differences of the mean fiber widths between the chrysotile and amphiboles, as measured in our study, seem to correlate well with the ratio of respirable and non-respirable fibers reported previously [Timbrell, 1970]. Cyclone measurement of the ratio of the respirable fraction in the anthophyllite was reported by Timbrell [1970] as being a little bit greater than in the other amphiboles, but the present data showed that the anthophyllite was greater in length and equal or thicker in width compared with the other amphiboles. Judging from these observations, the previous respirable fraction would have been affected by talc particles contaminating the anthophyllite sample. The present findings of the anthophyllite were obtained only from anthophyllite fibers, these fibers having been differentiated from talc particles (mostly platy and some fibrous) by their characteristic morphology, SAED pattern, and EDX spectrum.

DISCUSSION

The UICC asbestos samples have been very useful to many experimental studies on the health effects of asbestos. Well-characterized and easily available asbestos standards permit the comparison and assessment of results obtained by different groups. The reliability of the UICC asbestos samples has long been accepted. The samples were well characterized for some aspects when they were first introduced. However, complete and precise characterization of the mineral phases was not available. Our findings from state-of-the-art procedures may give rise to some confusion. For example, there was no tremolite found in chrysotile A; it would appear that in some reports [Wagner et al., 1986], the fibrous anthophyllite found in chrysotile A was believed to be fibrous tremolite. Another aspect concerns the purity of each sample. Chrysotile A and B samples were found to have fiber contents of 94 and 92%, respectively; they contained other minerals as impurities. The UICC anthophyllite sample now appears to be low in fiber content, approximately 60%. These observations may require reevaluations.

We detected some minor mineral phases at approximately 0.5% levels in the UICC asbestos samples in this study, and the quantification limit was estimated as approximately 1%. For amphiboles in chrysotile A and B, we examined at the 0.1% level using a highly sensitive XRD analysis. Chlorite minerals coexisted in both chrysotile A and B, and hydromagnesite in chrysotile B was close to the detection limit, indicated as "trace" in Table II. Chlorite particles were also identified by the ATEM observation. The thermal analysis using DTG clearly detected the weight

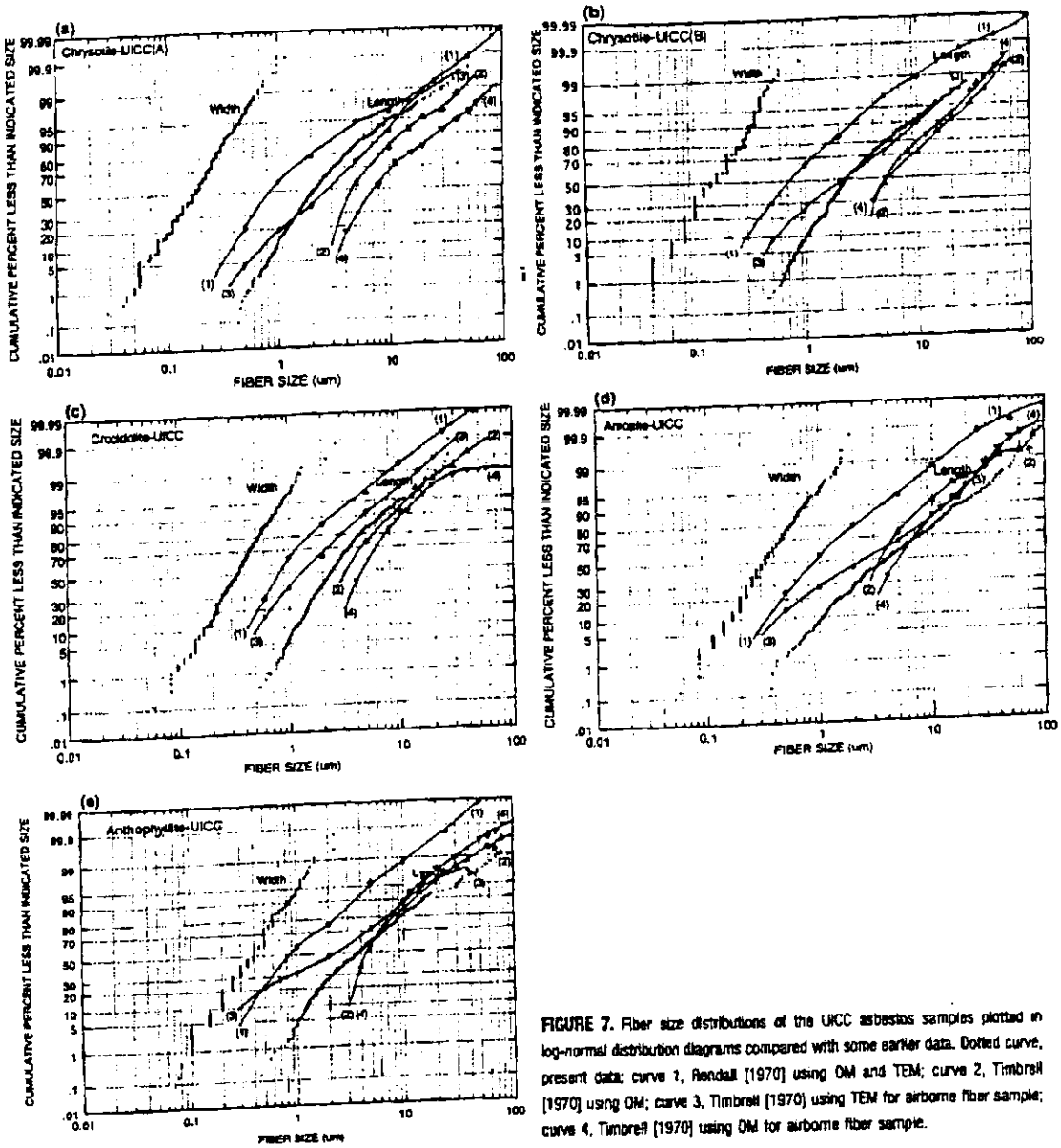

FIGURE 7. Fiber size distributions of the UICC asbestos samples plotted in log-normal distribution diagrams compared with some earlier data. Dotted curve, present data; curve 1, Rendall [1970] using OM and TEM; curve 2, Timbrell [1970] using OM; curve 3, Timbrell [1970] using TEM for airborne fiber sample; curve 4, Timbrell [1970] using OM for airborne fiber sample.

loss peak due to the dehydroxidation of hydroxyl water of chlorite at approximately 580°C. It has been demonstrated that DTG analysis is very effective for the quantification of minerals such as chlorite, brucite, and pyroaurite, when they have a lot of hydroxyl water and the detection limit sometimes exceeds that of XRD. Since DTG analysis is less useful for qualitative analysis than XRD analysis, DTG analysis is best utilized in conjunction with XRD and/or ATEM.

Chrysotile A from the Zimbabwe mine contains fibrous anthophyllite estimated at approximately 2%. Based on our unpublished data, most of the commercial chrysotile sam-

TABLE IV. Fiber Size Parameters of the UICC Standard Asbestos Samples*

	Length		Width	
	Mean (μm)	SD	Mean (μm)	SD
Chrysotile A	2.4	2.3	0.17	1.8
Chrysotile B	2.6	2.3	0.15	1.8
Amosite	4.3	3.3	0.31	1.9
	(2.8)	(1.9)	(0.30)	(1.6)
Crocidolite	2.5	2.0	0.33	2.1
	(2.9)	(1.9)	(0.25)	(1.6)
Anthophyllite	4.2	3.3	0.38	1.8

*Mean, geometrical mean; SD, geometrical standard deviation. Numbers in parentheses represent the second measurement.

ples from Zimbabwe (which were milled, and sent to Japan) contained fibrous anthophyllite in approximate amounts of the UICC chrysotile A. This means that the chrysotile from the Zimbabwe mine contained anthophyllite fibers which could not be separated by an industrial milling process. Visibly, the raw chrysotile fibers from the Zimbabwe mine seem to be harsh like amosite fibers. This implies that Zimbabwe chrysotile could be geologically produced at relatively higher temperatures, in which both chrysotile and anthophyllite could exist as stable states.

In some studies of carcinogenicity of fibrous anthophyllite, extremely high incidences of mesothelioma were observed in animal experiments in which this fiber type was injected directly into the peritoneal cavity of rats [Fukuda and Kohyama, 1995; Adachi et al., 1995]. On the other hand, information on cancer among employees of anthophyllite mines is relatively limited. In Finland, pleural calcification was first found in habitants near an anthophyllite mine by Kiviluoto [1960]. Meurman et al. [1974] reported a relatively high incidence of asbestosis, a significant increase in incidence of lung cancer, but no incidence of mesothelioma in the workers of a Finnish anthophyllite mine. Recently, the incidence of lung cancer and mesothelioma among the anthophyllite mine workers has been updated; 3 pleural and 1 peritoneal mesothelioma have been observed among 503 deaths of the 999-miner cohort [Meurman et al., 1994; Karjalainen et al., 1994]. A high incidence of pleural plaque was also found in the residents who had lived near an old anthophyllite mine and milling factory in Kumamoto prefecture, Japan [Hiraoka et al., 1990, 1992]. The mine and factory had been operated for about 20 years, since the early 1940s.

In 1991, Cullen and Baloyi [1991] assessed the data for asbestos-related diseases that had been found among chrysotile miners in Zimbabwe from 1980 to 1990. Their findings, acknowledged to be based on sparse data, supported the patterns of asbestosis, non-malignant respiratory disease, malignant mesothelioma, and lung cancer that have been reported elsewhere. Therefore, it is of interest to determine whether the incidence of lung cancer and mesothelioma in the Zimbabwe chrysotile miners and millers is significantly higher than among the other chrysotile miners who work with uncontaminated fibers. If a high incidence is observed, the anthophyllite fibers contaminating the chrysotile could have contributed to the incidence of lung cancer and/or mesothelioma. If the high incidence is not observed, it may be concluded that such a small contamination of anthophyllite fibers has no effect on the incidence of lung cancer and/or mesothelioma. Therefore, further epidemiological study of the miners and millers in the Zimbabwe chrysotile mine is necessary to assess the effect of such a low level contamination of amphibole asbestos (tremolite or anthophyllite) in chrysotile.

Fibrous anthophyllite was found in chrysotile A, but no amphibole asbestos was found in chrysotile B at the detection level of 0.1%. Wagner [1974] reported that most of the asbestos-related diseases, such as asbestosis, lung cancer, and mesothelioma, occurred in rats when they inhaled chrysotile B but no mesothelioma occurred due to chrysotile A; i.e., chrysotile A (containing anthophyllite fibers as impurity) could not induce mesothelioma. It is interesting to speculate as to why this difference occurred. Generally, such discrepancy is supposed to be within experimental error because the incidence of mesothelioma is very low as induced by inhalation experiments in animals. However, at least it can be said that the effect of the fibrous anthophyllite occurring in such a small amount was not larger than that of the chrysotile itself, which was the main component of the sample.

Kohyama and Suzuki [1991] reported the size distribution and contents of asbestos fibers (mostly chrysotile and amosite) in the lungs of North American insulation workers. The chrysotile and amosite that the workers used were mostly imported from Canada and South Africa, respectively [Selikoff et al., 1979]. The Canadian chrysotile and South African amosite could be considered to be almost the same as UICC chrysotile B and amosite, respectively. When we compared the size distributions of the two kinds of asbestos fibers found in the lungs with those of UICC chrysotile B and amosite, it was clearly shown that both kinds of asbestos fibers in the lungs were shorter and thinner than UICC chrysotile B and amosite, approximately one half in length and one third in width. This phenomenon can be explained by a size selection after inhalation; i.e., the larger fibers were selectively trapped at the upper tracheal tree and relatively fine fibers were deposited in the lung parenchyma. Moreover, fiber separation from fiber bundles into fibrils and dissolution of fibers probably occurred in the case of the inhaled chrysotile.

ACKNOWLEDGMENTS

We express sincere thanks to Dr. Wen-An Chiou of the Department of Materials Science and Engineering, Northwestern University, Evanston, IL, Mr. Steven R. Yuen of the Department of Community Medicine, Division of Environmental and Occupational Medicine, Mount Sinai School of Medicine, New York, NY, and Ms. S. Kurimori of the National Institute of Industrial Health, Ministry of Labour, Kawasaki, Japan, for their help with the preparation of this paper.

REFERENCES

Adachi S, Takemoto K, Hiraoka T (1995): Animal experiments for asbestos from Kumamoto, Japan. J Occup Health 37(Suppl):518 (in Japanese).

Bogovski P, Gilson JC, Timbrell V, Wagner JC (1973): "Biological Effects of Asbestos IARC Scientific Publication No. 8. Lyon: International Agency for Research on Cancer.

Cullen MR, Baloyi RS (1991): Chrysotile asbestos and health in Zimbabwe: I. Analysis of miners and millers compensated for asbestos related diseases since independence (1980). Am J Ind Med 19:161–169.

Fukuda K, Kohyama N (1995): Carcinogenicity of some fibrous minerals examined by peritoneal injections in rats. J Occup Health 37(Suppl):527 (in Japanese).

Graf JL, Draftz RG, Haartz JC (1982): Asbestos reference materials: Sources and characteristics. Proceedings of the NBS/EPA Asbestos Standards Workshop. NBS Special Publication No. 619, pp 5–20.

Hiraoka T, Kiyota S, Shima K, Kinuwaki E, Kimura T, Fukuda K, Shimazu K, Teshima Y, Izumi K, Fukuda Y, Numba K, Kuwahara T, Tanaka F, Hirota Y, Tamaru I (1990): Analysis of pleural plaque found at lung cancer screening examination. Jpn J Lung Dis 28:1566–1573.

Hiraoka T, Hiro Y, Shimazu K, Ohkura M, Teshima Y, Setoguchi K (1992): Endemic pleural plaques among the inhabitants around the asbestos mines and factories. Iryo 46:603–610.

International Union Against Cancer (UICC) Geographical Pathology Committee (1965): Report and recommendations of working group on asbestos and cancer: Relating to physics and chemistry. Ann NY Acad Sci 132: 720–721.

Karjalainen A, Meurman LO, Pukkala E (1994): Four cases of mesothelioma among Finnish anthophyllite miners. Occup Environ Med 51:212–215.

Kiviluoto R (1960): Pleural calcification as a roentgenologic sign of non-occupational endemic anthophyllite-asbestosis. Acta Radiol Suppl 194:1–67.

Kohyama N, Suzuki Y (1991): Analysis of asbestos fibers in lung parenchyma, pleural plaques, and mesothelioma tissues of North American insulation workers. Ann NY Acad Sci 643:27–52.

Meurman LO, Kiviluoto R, Hakama N (1974): Mortality and morbidity among the working population of anthophyllite asbestos miners in Finland. Br J Ind Med 31:105–112.

Meurman LO, Pukkala E, Hakama M (1994): Incidence of cancer among anthophyllite asbestos miners in Finland. Occup Environ Med 51:421–425.

Rendall REG (1970): The data sheets on the chemical and physical properties of the UICC standard reference samples. In Shapiro HA (ed): "Pneumoconiosis Proceedings of the International Conference, 1969, Johannesburg." Oxford: Oxford University Press, pp 23–27.

Rohl AN, Langer M (1974): Identification and quantitation of asbestos in talc. Environ Health Perspect 9:95–109.

Selikoff IJ, Hammond EC, Seidman H (1979): Mortality experience of insulation workers in the United States and Canada, 1943–1976. Ann NY Acad Sci 330:91–116.

Timbrell V (1970): Characteristics of the International Union Against Cancer Standard reference samples of asbestos. In Shapiro HA (ed): "Pneumoconiosis Proceedings of the International Conference, 1969, Johannesburg." Oxford: Oxford University Press, pp 28–36.

Timbrell V, Rendall REG (1972): Preparation of the UICC standard reference samples of asbestos. Powder Technol 5:279–287.

Wagner JC, Berry G, Timbrell V (1973): Mesothelioma in rats after inoculation with asbestos and other materials. Br J Cancer 28:173–185.

Wagner JC, Berry G, Skidmore W, Timbrell V (1974): The effects of inhalation of asbestos in rats. Br J Cancer 29:252–269.

Wagner JC, Chamberlain M, Brown RC, Berry G, Pooley FD, Davies R, Griffiths DM (1982): Biological effects of tremolite. Br J Cancer 45:352–360.

Wagner JC, Griffiths DM, Munday DE (1986): Recent investigations in animals and humans. In Wagner JC (ed): "The Biological Effects Of chrysotile. Accomplishments in Oncology. Vol 1, No. 2." pp 111–120.